SAE TECHNICAL
PAPER SERIES

960129

A New Closing Method for Wall Flow Diesel Particulate Filters

Per Stobbe and Henrik Guldberg Petersen
No Tox Corp.

Spencer C. Sorenson and Jakob W. Høj
Technical University of Denmark

**Reprinted from: Diesel Exhaust Aftertreatment 1996
(SP-1140)**

SAE The Engineering Society For Advancing Mobility Land Sea Air and Space®
INTERNATIONAL

**International Congress & Exposition
Detroit, Michigan
February 26-29, 1996**

400 Commonwealth Drive, Warrendale, PA 15096-0001 U.S.A. Tel: (412)776-4841 Fax:(412)776-5760

960129

A New Closing Method for Wall Flow Diesel Particulate Filters

Per Stobbe and Henrik Guldberg Petersen
No Tox Corp.

Spencer C. Sorenson and Jakob W. Høj
Technical University of Denmark

ABSTRACT

A new method has been developed to close the ends of a wall flow filter used for removing particulate matter from diesel engine exhaust. In this method, the ends of the honeycomb structure are capped by deforming and closing the ends of the channel walls between the extrusion and firing stages of production.

The method increases the amount of filtration area per filter volume for a given cell geometry conpared to the traditional plugging method, since the entire length of the honeycomb channels is used for filtration purposes. In addition, use of the capping method has a beneficial effect on the pressure loss characteristics of a filter with a given filtration area. These benefits are illustrated through experimental results.

INTRODUCTION

The wall flow filter has been used as a device to remove particulate matter from the exhaust of diesel engines (1). The original design of the wall flow filter consisted of an extruded honeycomb construction with alternate ends plugged by inserting and firing a plug in the appropriate channels.

Recent developments in the area of wall-flow filters have included the use of Silicon Carbide (SiC) as the base material for the filter structure (2). SiC has been shown to have advantageous properties as a filter material, including good strength, high thermal conductivity, high melting/decomposition temperature, and good permeability (3,4,5,6).

CHANNEL CLOSING

In connection with the development of SiC wall flow filters, a new capping method has been developed for channel closing. In the original version of the wall flow filter, ceramic plugs were fired into the ends of the channels. In order to ensure adequate strength for the plugs to remain in place, plug lengths of approximately 0.5-1.5cm have typically been used. Because of the thickness of the plugs, they have a large flow resistance and do not actively participate in the filtration process.

The use of the plugs reduces the effective filtration length of the channel by twice the plug length. This is because the plug is in contact with one channel at the inlet end and the adjacent channel at the outlet end, thereby affecting the filtration in both channels. This reduces the ratio of the effective filtration area to the filter volume or weight.

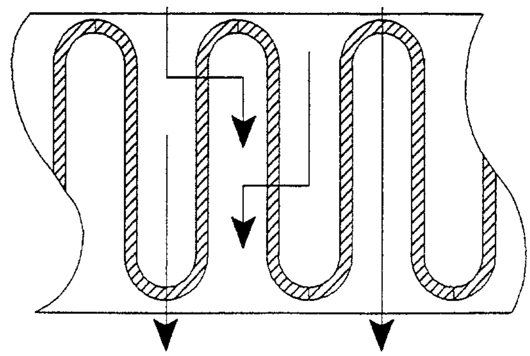

Figure 1. Schematic diagram of the filter capping technique.

The new capping method for channel closing consists of deforming the ends of the channel walls such that they are folded over until they are in contact with each other and form a cap. This is shown schematically in Figure 1. By using appropriate tools at the proper stage of the manufacturing process, the capping procedure has been readily accomplished for SiC wall flow filters.

With suitable deformation methods, it has been found possible to produce end caps without gaps, and with the same strength as the remainder of the filter body. The end capping technique is currently in production on all SiC filter bodies produced by the NoTox Corporation.

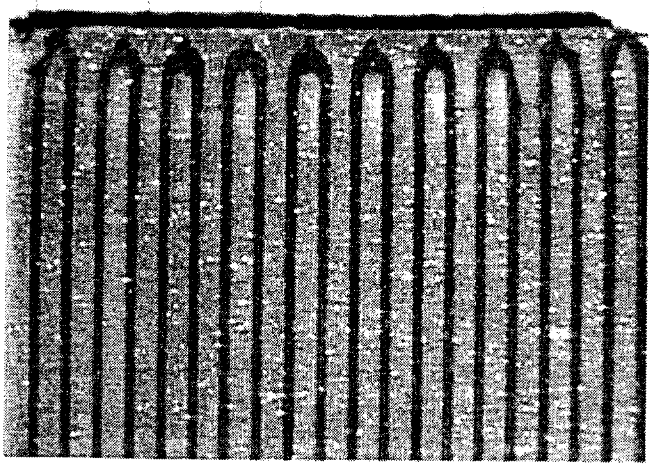

Figure 2. Cut away photograph of the side of a capped wall flow filter. The filter has been sliced along its longitudinal axis.

Figure 2 shows a photograph of a cross section of the ends of the channels in an SiC wall flow filter which has been constructed using the end capping method. It can be seen that the two ends have been folded in and joined in a tent-like construction. The joints at the sides of the walls where the ends have been deformed have been found to be leakage free after the final processing stages of the filter manufacture.

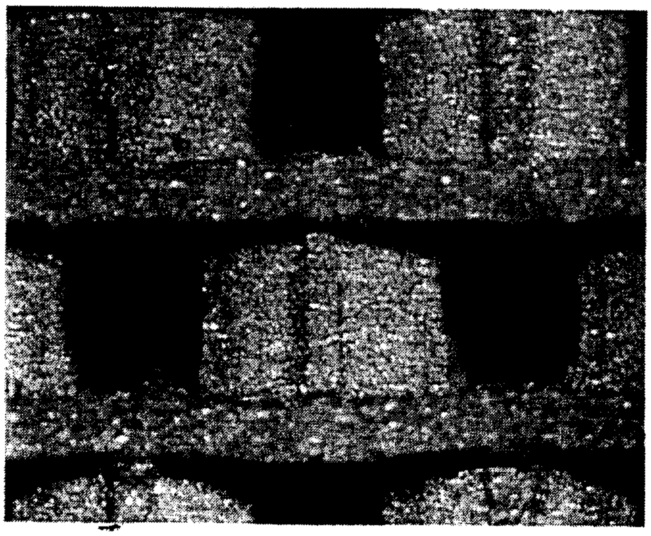

Figure 3. Photograph of the end of a wall flow diesel particulate filter which has been closed using the capping method.

Figure 3 shows a photograph of the end of a filter which has been closed using the production capping technique. It can be seen that the appearance of the ends of this filter is different than that of a conventional plugged filter. This is due to the angle of the cap. Figures 2 and 3 show that the entrance to the channels is of a more rounded nature than those of the plugged filters.

AREA/WEIGHT EFFECTS

The use of the capping method results in a significant reduction in the size and weight of filters for a given application, since a larger fraction of the total filter length is available for filtration purposes. In addition to reduction in the size, production costs are also reduced, due to a smaller amount of material consumption as well as less wear on the extruding equipment.

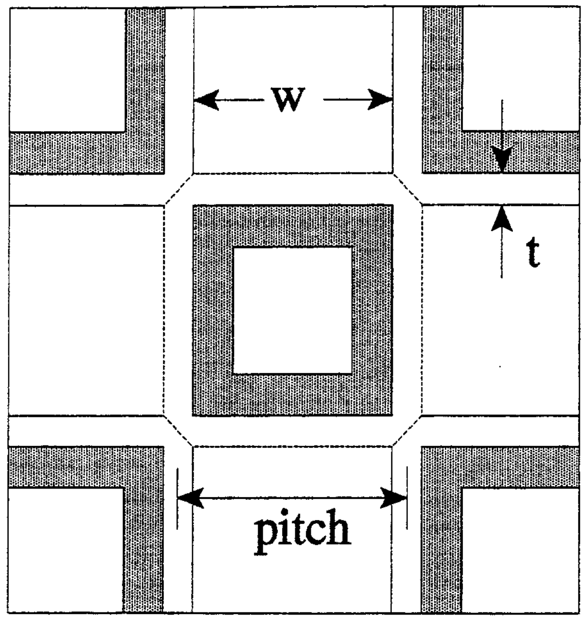

Figure 4. Geometry of the cross section of an extruded wall flow filter.

The reduction in filter size and weight is dependent on the geometry of the filter. The geometry of the channel cross section of a wall flow filter with square channels is shown in Figure 4, where P = the pitch of the channels, t is the wall thickness, and the open channel width, w is calculated as:

$$w = P - t \qquad (1)$$

When the ends of the channels are closed with the capping procedure, two of the sides are in essence folded in to form a tent-like closure. The geometry of this configuration is shown schematically in Figure 5. When the end is folded in, a portion of the side wall is lost to the filtration area, which is the area shown as area ABCD in Figure 5. On the other hand, the end area

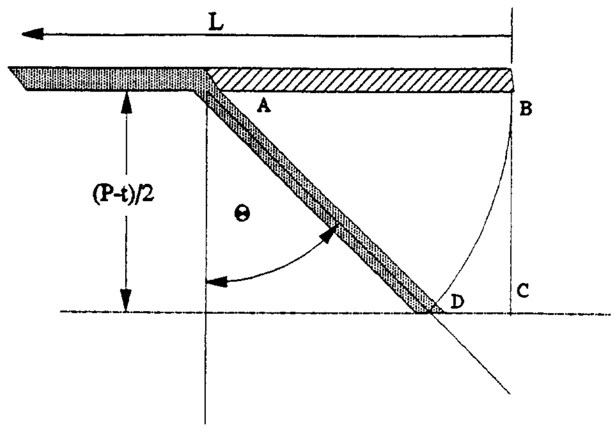

Figure 5. Geometrical representation of the capping procedure for wall flow filters.

which has been folded in remains a portion of the filtration area. The angle of the capped ends, θ in Figure 5, can be varied according to tooling used. This angle will have an effect on the filtration area, as shown in the following although for typical production values, the effect is quite small, as will be shown in the following.

For a given original length of an uncapped or unplugged filter honeycomb, the relationship between the area of a capped filter and a plugged filter can be determined by Equation 2, assuming that the capped and plugged filters have the same cross sectional area:

$$\frac{A_{cap}}{A_{plug}} = \frac{1 - \frac{(P-w)}{2L}\frac{1}{\cos(\theta)}}{\left(1 - \frac{2l_p}{L}\right)} \qquad (2)$$

where: A is filtration area, L is the uncapped/unplugged original length of the filter element, and l_p is the length of the plug in the filter.

Figure 6 shows the ratio of the filter areas as a function of plug length and filter element length for 15, 22, 30, and 45 cm filter elements. The base cell structure consists of a channel width, w = 2.0 mm and a wall thickness of 0.8 mm, and the capping angle, θ = 30°. The results show that the shorter the filter, the greater the area reduction caused by the plugging technique. Calculations for a filter with a channel width of 2.5 mm, wall thickness of 1.0 mm, and a capping angle of 30° show nearly identical results. Depending on filter length, improvement in filter utilization of between 5 to 15 percent is a realistic value for the benefit due to the capping procedure.

For short filters, the area loss due to plugging can be

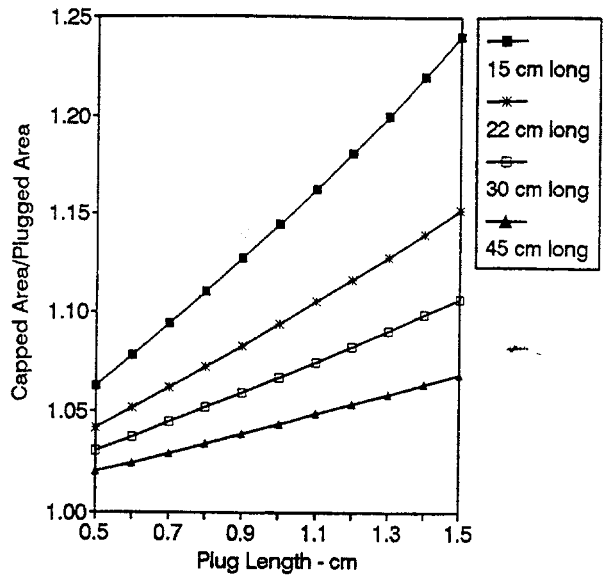

Figure 6. Effect of plug length on the ratio between the filtration area of a capped and plugged wall flow filter.

quite large for typical plug lengths. The shorter length of the capped filters increases the design flexibility in applications where especially length is critical.

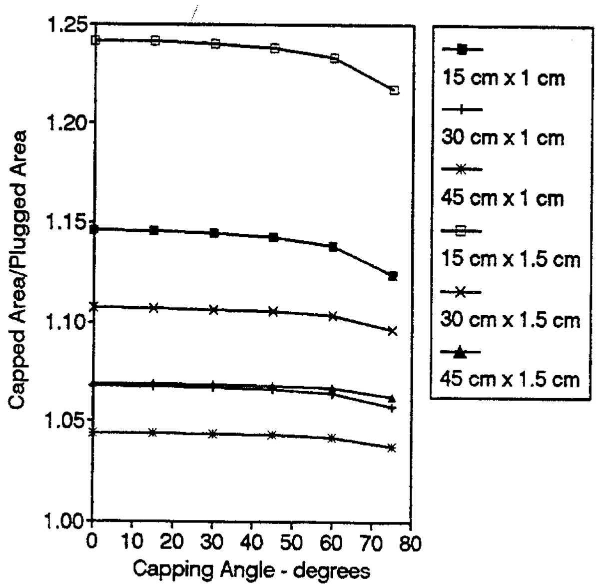

Figure 7. Effect of the capping angle on the ratio of filtration area for capped and plugged wall flow filters.

Figure 7 shows the effect of the capping angle on the ratio between the area of a capped filter and a plugged filter for a channel width of 2 mm, wall thickness of 0.8 mm, and lengths of 15, 30 and 45 cm. Calculations for a filter with a channel width of 2.5 mm, wall thickness of 1.0 mm and the same lengths give nearly identical results. The effect of the capping angle can be seen to be very small for capping angles up to 60°. Angles larger than this can be considered to be impractical from a production point of view and in practice, then, the effects of the capping angle on the filtration area of a capped filter can be ignored.

FLOW CHARACTERISTICS

There are different ways to compare the net effects of the capping method on pressure drop characteristics. In practice, the comparison should be made on the basis of the same effective filter length for both the capped and plugged filter elements. This will result in essentially the same pressure drop over the porous wall, but the pressure drop through the channels will be greater for the plugged filter, since it will have a longer channel.

Another option is to compare equal effective channel lengths of the plugged and capped filters. This results in a capped filter which has a larger filtration area that the plugged filter with a lower wall velocity and wall pressure drop, but the same expected pressure drop through the channel, since the flow lengths of the channels are the same. These samples were prepared with the same inlet channel length as the plugged filters. Given the complicated nature of the flow along the channel and through the walls, it is possible that this is not the correct channel length for equal pressure drops due to channel flow. In the final analysis, the most important comparison is between the plugged filters and the capped filters with the same filtration area, since this is the situation which will be encountered in a practical application.

Consequently, test samples with corresponding lengths were prepared for each of 4 combinations of 2 filter lengths and 2 channel geometries. The samples used for in the present experiment were all prepared from extruded honeycomb monoliths of SiC. The two channel size samples were prepared from the slightly different base SiC filter material (NF-820 for the 2 mm channels with 0.8 mm wall thickness, and NF-850 for the 2.5 mm channels with 1.0 mm wall thickness) and different extruders were used for the 2 sizes.

After extrusion of the filter bodies, samples were cut to desired length and the channels closed in the well-known checker board geometry using the two different closing methods: capping and plugging.

After extrusion, channel closing, and sintering, residual carbon from the manufacturing process was removed by heating in air. Data for the samples used in the experimental study are given in Table 1. Note that the effective filtration length is equal to the total length of the body minus 2 times the closure length:

Width mm	Thickness mm	Closure	L_{tot} mm	$L_{closure}$ mm	L_{eff} mm
2.0	0.8	Cap	99.8	2.6	94.6
2.0	0.8	Cap	105	3.0	98.8
2.0	0.8	Plug	112	7.1	97.7
2.5	1.0	Cap	101	4.0	93.2
2.5	1.0	Cap	106	4.5	97.3
2.5	1.0	Plug	112	7.2	97.1
2.0	0.8	Cap	204	2.7	199
2.0	0.8	Cap	208	2.9	202
2.0	0.8	Plug	214	6.9	201
2.5	1.0	Cap	203	3.3	196
2.5	1.0	Cap	209	3.2	202
2.5	1.0	Plug	213	7.6	199

Table 1. Data for the samples used for flow measurements.

$$L_{eff} = L_{tot} - 2\,L_{closure}.$$

A schematic representation of the geometries of these samples is shown in Figure 8.

Cold flow measurements were performed by testing the samples on a specially constructed flow bench. The flow

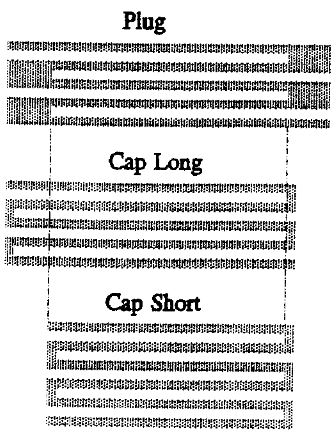

Figure 8. A schematic representation of the geometries of the capped and plugged filter samples as used for the flow characteristic testing.

rate was controlled from 0-150 m^3/hr (STP) by electrical control of the rotational speed of 3 centrifugal blowers. The flow rate was measured using a Meriam Laminar flow meter. The pressure drop is measured using an electric pressure transducer (0-500 mbar), calibrated against a U-tube manometer before performing the experiments.

The flow rate measured using the hot-wire air mass sensor is essentially independent of the gas temperature, but since there is a slight increase in gas temperature due to the centrifugal blower, the temperature of the gas was measured immediately after the sample using a PT100 thermocouple.

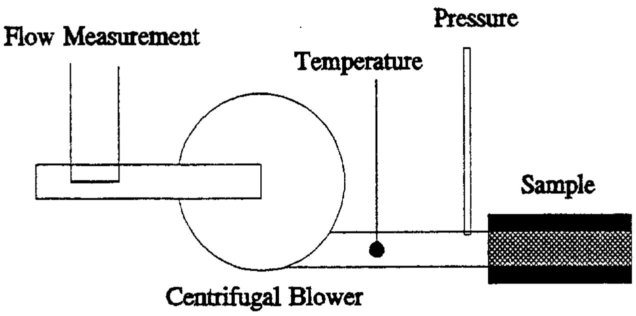

Figure 9. Schematic diagram of the experimental system used to measure the flow characteristics of wall flow filter samples.

The error was 1 m^3/hr and 10 Pa in the flow rate measurements and pressure measurements respectively. Figure 9 shows a schematic drawing of the flow bench setup.

For all samples, the outer wall was sealed air tight in order to prevent flow through the outer wall of the samples.

The background pressure drop due to loss in fittings was measured versus the flow rate, in the flow system without a filter element. A correlation was made of the these data in order to express the background pressure drop as a function of flow rate.

The results of the tests is shown in Figures 10 through 13. In these figures, the pressure drop across the samples is plotted as a function of the ratio of the flow rate to the filtration area. This was done in an attempt to compensate for the minor differences in the actual filtration area that arise during the construction of the samples. The ratio of the volumetric flow rate to the filtration area is, in fact, the face velocity at the filter. Assuming that the flow through the porous wall obeys

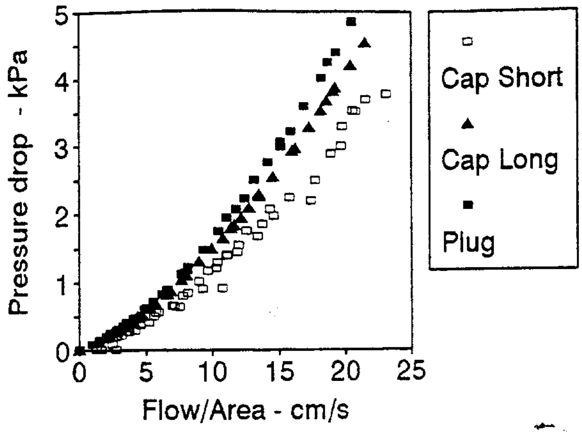

Figure 10. Pressure loss for filter samples, 100 mm x 2.0 mm x 0.8 mm.

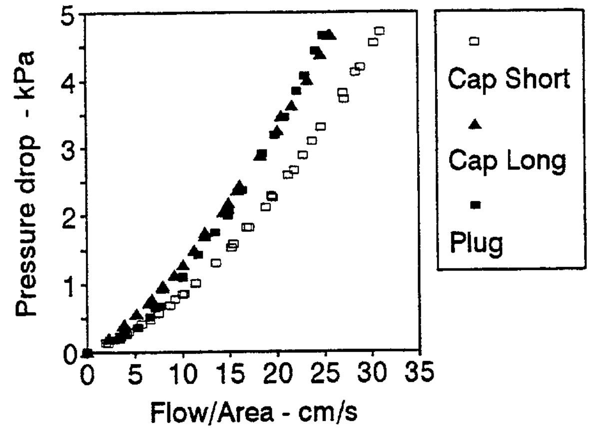

Figure 11. Pressure loss for filter samples, 200 mm x 2.0 mm x 0.8 mm.

Darcy's law and equal permeabilities and wall thicknesses, then for a given face velocity, the pressure drop through the wall should be the same, regardless of the plugging technique (7,8). Thus in principle, the effect of wall pressure drop is removed, assuming that the permeabilites of all samples within a set are equal.

Two curves are given for the capped filters. The first is denoted "Cap Long", and represents the situation where effective channel length of the capped and plugged filters is the same. This is the length through which fluid friction caused by flow through the channels acts on the gasses. In this case, the capped filter has a larger filtration area, and should have a lower pressure drop across the porous wall for the same flow rate.

The second is denoted as "Cap Short", in which the effective filtration area is the same as the plugged sample, but the flow channel is shorter by the length of a plug. Figure 8 shows the differences in the samples.

In all cases, the plugged filter samples give a greater

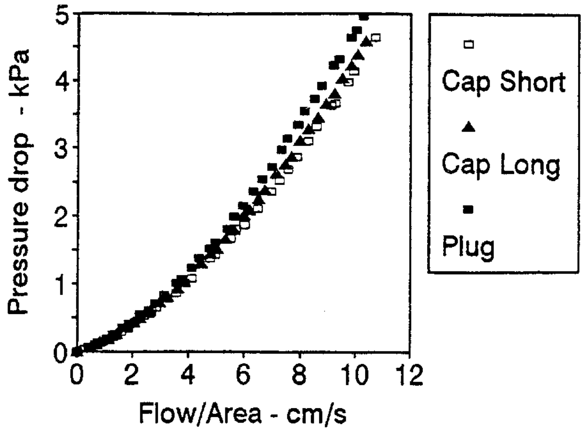

Figure 12. Pressure loss for filter samples, 100 mm x 2.5 mm x 1.0 mm.

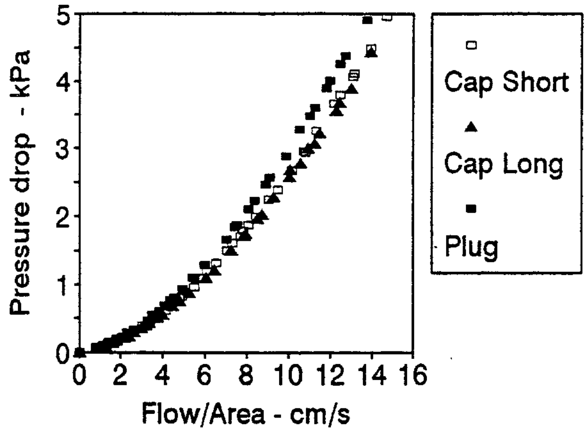

Figure 13. Pressure loss for filter samples, 200 mm x 2.5 mm x 1.0 mm.

pressure drop than the short capped filter samples. The pressure drop for the plugged filter samples is also greater than for the short capped filter sample of 100 mm x 2.5 mm x 1.0 mm as shown in Figure 11. Here the plugged and long capped filter samples give about the same pressure drop. For the 100 mm long samples seen in Figures 10 and 11, the short capped filter samples have lower pressure drops than the long capped samples.

It appears that the long capped sample with 2.5 mm channel and 1.0 mm wall thickness has a lower permeability, since at the lower flow rates the pressure drop for the long capped filter is the largest. This is the area of the flow where the wall flow contribution should be the largest. The curve for the long capped filter also has less curvature than the other curves, consistent with a higher relative contribution of the wall loss.

The results indicate that the use of the capping closure method results in lower pressure losses, and that these differences are largest at the highest flow rates. An interesting observation is that the long capped filters exhibit lower pressure drops than the plugged filters for a given filtration face velocity.

This is expected in the basis of the assumption that the pressure drop across the filter is due to the sum of the wall pressure drop and the channel drop. If one assumes that for flow through the channels has the following characteristics for turbulent flow (7):

$$f_w = K \cdot Re_w^{-a} \qquad (3)$$

where: f_w = friction factor for flow through the channel, and K and a are constants. The constant a is on the order of 0.25 to 0.35. The friction factor, f, is defined as:

$$f \equiv \frac{\Delta p \frac{d}{l}}{\rho \frac{v^2}{2}} \qquad (4)$$

Where: ρ is the gas density, d = P - t, l is the length of the channel, and v the axial velocity of the gasses entering the channel.
Then:

$$\Delta p = \frac{v_f t \mu}{\alpha} + K \frac{\rho v_f^2}{2} \left(\frac{4 \rho l_{eff} v_f}{\mu} \right)^{-a} \left(\frac{16 l_{eff}^2 l_{ch}}{w^3} \right) \qquad (5)$$

where: v_f is the filter face velocity, t is the wall thickness, μ is the viscosity, α is the permeability, ρ the gas density, and l_{eff} is the effective filtration length, and l_{ch} is the total length of the channel through which there is flow.

Note that a given filter face velocity does not necessarily imply the same flow rate. For the long capped filters in comparison with the plugged filters, for example, implies a larger flow rate, since the longer effective length (filtration area) of the capped filter requires more flow through it in order to maintain a given filter face velocity. The pressure drop through the wall, according to Darcy's equation (the first term on the right hand side of equation (5)), will be the same due to the same velocity, but the pipe flow contribution will be larger in the plugged sample due to the higher flow rate. This is reflected in last term in the parentheses in Equation (5), since it can be shown that l_{ch}/w is the ratio between the channel entrance velocity (flow rate per channel) and the filter face velocity.

Equation (5) shows that for the same channel length, and face velocity, the filter with the smallest effective filtration length has the smallest pressure drop. That is, it is expected that the long capped samples will have a lower pressure drop than the plugged samples, since the effective filtration length of the long capped samples is greater than that of the plugged samples.

The short capped filters should have the smallest pressure drops, since the effective filtration length is the same as the channel length, which for a plugged filter, the channel length is larger than the effective filtration length. All else equal, this should be the main source of pressure loss reduction when using capped filters instead of plugged filters.

It is of interest to note that the long capped filters give lower pressure drops than the plugged filters, which according to Equation (5) is not expected. Therefore, it is of interest to speculate as to whether there are other influences on the pressure losses.

END EFFECTS

One possibility is the effect of channel end geometry on the entrance and/or exit losses at the inlet/outlet faces of the filter. The photographs of the ends of the capped filters indicate that the capped filters have a more rounded end at the entrance and exit to the filter. Preliminary calculations on the basis or sudden expansion/contraction indicated that there was a possibility that observable effects on flow losses could be obtained simply due to the change of entrance geometry (9).

An additional series of tests was therefore conducted to investigate this further. In the tests of plugged filter samples, pressure losses should be dominated by two factors: the pressure drop through the porous walls, and the pressure loss due to the axial flow through the channels. In order to make a more accurate assessment of the effects of the ends of the channels, a special set of samples was constructed and tested.

In these samples, only one end of alternate channels was closed by either capping or plugging, and the outlet side was not closed at all. With such samples, the only significant pressure losses should be due to the effects of the flow through the channels and the closure method, as there should be little or no flow through the porous walls. This corresponds to a conventional filter which has one end cut off.

In the measurements, the friction factor was used to compare pressure losses, since this should compensate for small differences in geometry.

The Reynolds number is based on the flow through an average single channel and is calculated as:

$$Re_w = \frac{\dot{m}_g}{w \, \mu \, N_{channels}} \qquad (6)$$

Where: $\dot{m}_g$ is the total mass flow through the sample, μ is the viscosity, and $N_{channels}$ is the total number of open channels.

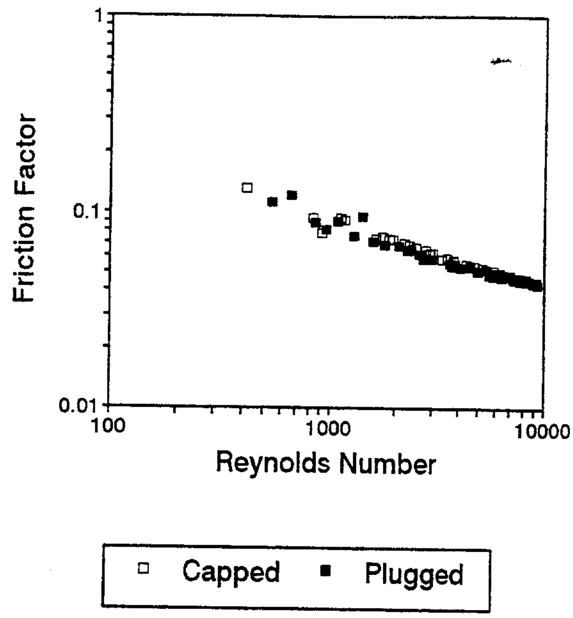

Figure 14. Friction factor as a function of Reynolds number for a filter sample: 100 mm x 2.5 mm x 1.0 mm with unplugged exit.

Figure 14 shows the results for flow through capped and plugged samples for a samples with a length of 100 mm a channel width of 2.5 mm and a wall thickness of 1.0 mm, while Figure 15 shows comparable results for a length of 200 mm, width of 2.0 mm and a wall thickness of 0.8 mm. These samples represent a range of l/w from 40 to 100.

It can be seen that within the accuracy of the experimental data, there is no measurable effect of the closing technique on end losses in the filters, even for a very short filter in the case where there is no pressure loss due to flow through the porous walls. In an actual filter, then, the relative effect of the end closing technique would be expected to be even smaller, since there would be a large contribution to the pressure drop by the flow through the wall.

The flow at the ends of actual filters may be somewhat different since there could be a small amount of flow through the end cap, since it is of the same thickness as the rest of the wall. The cap area comprises between

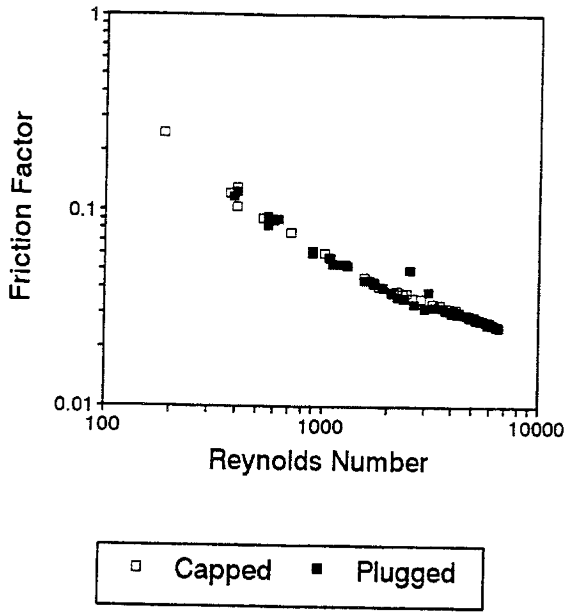

Figure 15. Friction factor as a function of Reynolds number for a filter sample: 200 mm x 2.0 mm x 0.8 mm with unplugged exit.

1.4 to 3.6 % of the total filtration area of the tested filter samples. This is slightly different situation than that which has been previously investigated (10). Regardless, it appears that the aerodynamic effects of the caps in their current form is quite small, and that the major benefit of the capped filters accrues from the shorter channel length per filtration area.

CONCLUSIONS

A new method for closing the ends of extruded wall flow diesel particulate filters has been presented. In the method, the ends of the filter channels are deformed before firing into a cap across the end of the channels. This cap consists of the same material as the rest of the filter, and contributes to the effective filtration area.

For typical plug and filter lengths, a reduction in filter volume and weight of 5 - 15 % can be achieved.

Use of the capping method results in reduced pressure loss across the filter compared to those occurring with the plugging method which has been prevalent earlier.

Direct geometrical effects of the capping technique on entrance pressure losses were not observed in tests with open channels, even though tests with actual filters closed on both ends suggest a minor benefit of the capping method.

REFERENCES

1. Howitt, J. S., Montierith, M. R., "Cellular Ceramic Diesel Particulate Filter", SAE paper 810114, 1981.

2. Stobbe, P., J. W. Høj, H. Pedersen, S. C. Sorenson, "SiC as a Substrate for Diesel Particulate Filters", SAE Transactions, Paper 932495, 1993.

3. S. C. Sorenson, J. W. Høj, P. Stobbe " Flow Characteristics of SiC Diesel Particulate Filter Materials", SAE Paper 940236, in Diesel Exhaust Aftertreatment 1994, SP-1020, SAE International 1994.

4. Høj, J., Sorenson, S. C. Sorenson, P. Stobbe, "Thermal Loading in SiC Particle Filters", SAE Paper 950151, 1995.

5. Itoh, A. et al. "Study of SiC Application to Diesel Particulate Filter (Part 1): Material Development", SAE paper 930360.

6. Itoh, A. et al. "Study of SiC Application to Diesel Particulate Filter (Part 2): Engine Test Results", SAE paper 930360.

7. Bird, R. B., W. E. Stewart, and E. N. Lightfoot, Transport Phenomena, Wiley and Sons, New York, 1960.

8. Meyer, B.A. and Smith, D.W. "Flow Through Porous Media: Comparison of Consolidated and Unconsolidated Materials", Ind. Eng. Chem. Fundam., 24, 360-368, 1985):

9. Dullien, F. A. L. Porous Media Fluid Transport and Pore Structure, Academic Press, Inc., New York, 1979.

10. Konstandopoulos, A. G. and J. H. Johnson, "Wall-Flow Diesel Particulate Filters--Their Pressure Drop and Collection Efficiency", SAE Paper 890405, in Developments in Diesel Particulate Control Systems, SAE Special Publication SP-775, 1989.